Journal Name

ARTICLE

Transformation of Worst Weed into N-, S-, and P-tridoped Carbon Nanorings as Metal-Free Electrocatalysts for Oxygen Reduction Reaction

Received 00th January 20xx,
Accepted 00th January 20xx

DOI: 10.1039/x0xx00000x

www.rsc.org/

Shuyan Gao, [a]* Xianjun Wei,[a] Haiying Liu,[b] Keran Geng,[a] Hongqiang Wang, [c,d]* Helmuth Moehwald[e] and Dmitry Shchukin[d]

Substituting sustainable/cost-effective catalysts for scarce and costly metal ones is currently among the major targets of sustainable chemistry. Herein we report the synthesis of N-, S-, and P-tridoped, worst-weed-derived carbon nanorings (WWCNRs) that can serve as metal-free and selective electrocatalyst for the oxygen reduction reaction (ORR). The WWCNRs are synthesized via activation-free polymerization of worst weed, Eclipta prostrate, and then removal of the metallic residues by HCl. The WWCNRs exhibit good catalytic activity towards the 4 electron-transfer ORR with low onset potential and high kinetic limiting current density, along with high selectivity (introducing CO, the sample loses only <7% of its original activity, in contrast to more than 30% loss of the original activity for 20 wt% Pt/C over 4000 s of the continuous ORR) and long durability (94% of the initial current still persists at the sample electrode compared with a 87% current retention at commercial Pt/C electrodes after 18,000 s). The present work highlights the smart transformation of organic-rich worst weed into value-added functional materials with great potential in applications such as fuel cells, lithium–air batteries, photocatalysis, and heterocatalysis.

Introduction

The oxygen reduction reaction (ORR) is a key process in energy storage and conversion, notable examples of which includemetal–air batteries[1] and fuel cells,[2] where the sluggish kinetics of ORR seriously hinders the overall development.[3,4] Therefore, great efforts have been devoted to exploiting catalysts to boost the performance. Currently, platinum (Pt)[5,6] and Pt-based[7-12] catalysts are common for ORR. However, the limited global abundance, generally high price, poor stability, and intolerance to fuel crossover, represent vital problems for exploitation of Pt and Pt-based catalysts.[2] Hence inexpensive and sustainable catalysts are crucially needed to make the ORR-related technology widely applicable.[13] As an important example, heteroatom-doped carbon materials have particularly attracted considerable attention due to their low cost, excellent ORR electroactivity, long-term stability, and excellent immunity to methanol crossover and CO poisoning.[19,21–25] For example, B,[26-28] N,[29-34] P,[35-38] and S[39-42] doped carbon materials have been one of the most active research topics because heteroatoms make the catalysts non-electron-neutral, thereby facilitating the adsorption of oxygen and the subsequent reduction of oxygen.[22,43,44] Both theoretical calculation and experimental results have proved that heteroatom (N, P, S etc.) doped carbonaceous materials exhibit unusual physical and electrochemical properties, which have drawn extensive attention as potential metal-free catalysts for oxygen reduction reaction (ORR) in the past decades.[37,45] Nitrogen doped carbons are the most studied carbon-based catalysts for the ORR.[46] Nitrogen, an electron donor, can provide n-doping and therefore increases the conductivity of carbon. Furthermore, doping of carbon with N induces electronic structure changes (charge redistribution and charged sites (C+) creation) as well as structural changes (edge-active sites), which are reported to contribute to the enhancement of kinetics of the ORR. Compared to N, phosphorus (P) as one of the N-group elements also becomes an alternative because the P-doping induces defects in the carbon framework and increases the electron delocalization due to good electron donating properties of P, promoting active sites for ORR.[35,47] Additional P-doping induces uneven and wrinkled surfaces with the open edge sites split and angled. Moreover, surface area expansion resulting from the P doping has positive effects on the ORR activity of the catalysts.[48] As for the S-doped metal-free electrocatalysts for

[a] Collaborative Innovation Center of Henan Province for Green Manufacturing of Fine Chemicals, School of Chemistry and Chemical Engineering Henan Normal University, Xinxiang 453007, Henan, China. E-mail: shuyangao@htu.cn
[b] School of Life and Life Sciencest, Henan Normal University, Xinxiang 453007, Henan, China.
[c] State Key Laboratory of Solidification Processing, Center for Nano Energy Materials, School of Materials Science and Engineering, Northwestern Polytechnical University, Xi'an 710072, China
E-mail: Hongqiang.Wang@nwpu.edu.cn
[d] Stephenson Institute for Renewable Energy, Department of Chemistry University of Liverpool, Crown Street, Liverpool, L69 7ZD, UK.
[e] Department of Interfaces, Max Planck Institute of Colloids and Interfaces, Am Mühlenberg 1, 14424 Potsdam-Golm
† Supporting information for this article is given via a link at the end of the document.((Please delete this text if not appropriate))

ORR, research has mainly focused on the investigation of S-doped carbon materials with graphite-like structure. Theoretically, Denis et al. predicted that S-doping in graphene is feasible for ORR, although it is not as good as the nitrogen doping. The influence of the doped sulfur atoms on the spin density, polarisability, and structural defects could significantly improve the ORR performance of these carbon-based metal-free electrocatalysts.[49,50] It is clear that unary N-doped, S-doped or P-doped carbon shows good performance in enhanced activity for ORR. However, unary doping of heteroatom into carbon material as catalyst have exhibited much lower ORR activities than those of binary and ternary doping catalysts.[51] Thence, binary and ternary heteroatom doping will be a better choice to synthesize cathode catalysts with high ORR activity. For example, S-doping into the N-doped carbons can cause activity nearly 2.5 times higher than that of solely N-doped carbon.[52] In fact, not only binary S/N- but also ternary P/S/N-doping results in enhanced activity for ORR.[52] The binary and ternary doping of P and/or S in N-doped carbon produces many edge sites and a high surface curvature. The increase in activity obtained via the additional doping of P and S into N-doped carbons results from the enhanced asymmetry of the atomic spin or charge density, which provides the O_2-sorption sites. However, methods used for doped carbon materials preparation often involve tedious chemical vapor deposition (CVD) and/or hazardous to environment methods. Furthermore, multi-heteroatoms doping carbon materials for ORR remain largely unexplored so far.[47,52] Taking fully into account the enormous potential of tridoped metal-free carbon materials, it is a great and challenging task to produce tridoped metal-free carbon-based ORR electrocatalysts, especially from an economical and sustainable viewpoint. Following this idea, we herein report the facile synthesis of N-, S- and P-tridoped carbon nanorings from worst weed, *Eclipta prostrata* (named worst weed-derived carbon nanorings, WWCNRs) with efficient ORR electrocatalytic performance.

Experimental section

Methods synthesis

Eclipta prostrate was reaped from author Prof. Haiying Liu's experimental field. After removing the roots and washing with deionized water, it dried naturally under ambient condition for further use. For the synthesis of WWCNRs, 10 g of thoroughly dried Eclipta prostrata was heated in an alumina crucible put in a quartz tube at 800°C under a N_2 atmosphere for 2 h with a heating rate of 10 °C min^{-1}. After naturally cooling, the black powder was put in 20 ml 2.0 M HCl solution for 12 h at room temperature, filtered and washed with hot deionized water to remove metallic components, and dried at 40°C overnight.

Characterization

The TEM and HRTEM images were taken with a JEOL FE-2010 microscope operated at an accelerating voltage of 200 kV. The powder XRD patterns were recorded on a Bruker-D8 apparatus with Cu Kα radiation (λ = 1.54060 Å) at a scan rate of 2° min^{-1}. Corresponding work voltage and current is 40 kV and 100 mA, respectively. XPS was recorded by a scanning X-ray microprobe (PHI 5000 Verasa, ULAC-PHI, Inc.) using a monochromic Al X-ray source and the C_{1s} peak at 284.6 eV as internal standard. The Raman spectra were obtained on a Renishaw inVia unit with excitation at 514.5 nm by an argon ion laser. The N_2 adsorption-desorption experiments were performed at 77 K using a Micromeritics ASAP 2020-Physisorption Analyzer (Micromeritics, USA). Prior to the measurement, all samples were degassed at 350 °C for 12 h until the pressure was less than 5×10^{-3} Torr. The BET method was used for surface area determination.

Electrochemical measurements

All electrochemical experiments were conducted on a CHI660D electrochemical station (Shanghai Chenhua Co., China) in a standard three-electrode cell equipped with gas-flow systems at room temperature. A piece of Pt foil served as the counter electrode. The Hg/HgO reference electrode was placed in a separate chamber and located near the working electrode chamber through a Luggin capillary tube.

The preparation procedures of GC electrodes were as follows: prior to use, the electrodes were polished mechanically to a mirror finish with aluminite power under a chamois, successively washed with ethanol and deionized water to remove any bound particles, and dried under a gentle air stream. 10 μL (8.33 mg/mL) well-dispersed catalyst prepared by sonicating the mixture of 1 mg of the catalysts, 100 μL deionized water, and 20 μL of solvent of Nafion (5%) were pipetted onto the GC electrode surface and allowed to dry under ambient condition. For comparison a commercially available Pt/C (20 wt%, Johnson Matthey) catalyst was prepared using the same electrode configuration in the same way.

For ORR measurements, CVs were measured at room temperature from −0.8 to 0.2 V at a scan rate of 10 mV s^{-1} in 0.1 M KOH solution bubbled with N_2 or O_2 for at least 30 minutes in advance. In the RDE test, LSVs were measured in O_2-saturated 0.1 M KOH solution and the potential was varied from 0.4 to −0.8 V with a scan rate of 10 mV s^{-1} at various rotating speeds from 400 to 2025 rpm.

To evaluate the ORR performance, the number of transferred electrons (n) was analyzed at various potentials according to the K-L equation:

$$\frac{1}{J}=\frac{1}{J_L}+\frac{1}{J_K}=\frac{1}{B\omega^{1/2}}+\frac{1}{J_K} \quad (1)$$

$$B=0.62nFC_0D^{2/3}\nu^{-1/6} \quad (2)$$

where J, J_k, and J_L are the measured, kinetic, and diffusion-limiting current density, respectively. B is the Levich slope given by (2), n is the number of transferred electrons for ORR. ω is the rotation speed (ω = 2 πN, N is the linear rotation rate), F is the Faraday constant (F = 96485 C mol^{-1}), ν is the kinetic viscosity (ν = 0.01 cm^2 s^{-1}), and CO_2 is the concentration of O_2 in the solution (1.2×10^{-3} mol L^{-1}), and D_{O2} is the diffusion coefficient of O_2 in 0.1 M KOH (1.9×10^{-5}

cm^2 s^{-1}). The constant 0.2 is adopted when the rotation speed is expressed in rpm.

The methanol tolerance test was conducted in O_2-saturated 0.1 M KOH in the presence and absence of methanol in the potential range from –0.8 V to +0.2 V at a scan rate of 10 mV s^{-1} at room temperature. The CO poisoning and stability of the sample catalyst was assessed by the current-time (i-t) chronoamperometric response in O_2-saturated 0.1 M KOH. Fresh electrolyte solution (0.1 M KOH aqueous solution) was used for each electrochemical measurement to guarantee reproducible results. All potentials displayed herein are given versus Hg/HgO (1 M KOH) electrode.

Results and discussion

The plant, *Eclipta prostrata*, is a member of the Asteraceae plant family and commonly known as worst weed in rice field or paddy field. Earlier literature surveyed on the plant revealed that the major compounds isolated from *Eclipta prostrata* were volatile components like, flavonoid, isoflavonoids and coumestan.[53] *Eclipta prostrata* and *Eclipta alba* are rich in flavonoids broadly belonging to the class of phenolic compounds.[54] Preparation of N-, S- and P-tridoped WWCNRs was accomplished by direct pyrolysis of Eclipta prostrata under nitrogen atmosphere at 800 ^{o}C and washing in HCl.The detailed schematic depiction of the synthesis is shown in was accomplished by direct pyrolysis of Eclipta prostrata under nitrogen atmosphere at 800 ^{o}C and washing in HCl. The detailed schematic depiction of the synthesis is shown in Scheme 1. The obtained carbon powder is black and from transmission electron microscopy (TEM) images appears as intercrossing nanorings as shown in Fig. S1, suggesting the porous nature of the resulting materials. The high-resolution TEM (HRTEM) image (Fig. 1A), validates the intercrossing state of WWCNRs much clearer. At the same time, the observed lattice spacing of 0.345 nm is in accordance with the interlayer distance of graphite. X-ray diffraction (XRD, Fig. 1B) measurement of the sample reveals that the product exhibits two peaks at 2θ = 25° and 44°, which can be attributed to the (002) and (101) planes of hexagonal graphite (JCPDS card no. 41-1487), respectively.[55,56] The corresponding d-spacing is calculated to be 3.45 Å. This slight shift in the (002) peak and the increased d-spacing observed in the sample imply a lower graphitic ordering in the sample. This can be attributed to the distortion as a result of the heteroatom-incorporation.[57,58] In order to further investigate the structural information, Raman D- and G-band intensities were used to characterize the carbon materials, particularly analyze the crystallization degree of graphitic carbon. A typical D-band at roughly 1363 cm^{-1} attributed to an A_{1g} vibration mode of carbon atoms with dangling bonds in plane terminations of disorder graphite and a G-band at 1597 cm^{-1} associated with the vibration of sp^2- hybridized graphitic carbon atoms can be in Fig. 1C, respectively.[40,59,60]

The survey scan of the sample (Fig. 2A) shows an identical elemental composition (C_{1s}, N_{1s}, O_{1s}, S_{2p}, P_{2p}), suggesting that N-, S- and P-heteroatoms were successfully doped into the sample. The high resolution spectrum of N_{1s} (Fig. 2B) can be divided into three peaks, corresponding to graphitic N (~401.2 eV), pyrrolic N (~399.8 eV) and pyridinic N (~398.6 eV),[60] respectively. The graphitic and pyridinic N are assumed to be more ORR active.[61] The P2p peak at approximately 132.0 eV in Fig. 2C is attributed to the P-C bonding.[35] In addition, the $S_{2p\ 3/2}$ (163.8 eV) and $S_{2p\ 1/2}$ (164.8 eV) peaks are ascribed to sulphide groups (-C-S-C) (Fig. 2D).[62] Remarkably, the sample contains sulfur atoms that form thiophene-like structures with neighboring carbon atoms, as shown in the high-resolution S_{2p} spectrum. The -C-SOx-C peak (168.5 eV) is also observed in Fig. 2D, which is chemically inactive for ORR.[26] The high-resolution spectrum of C_{1s} (Fig. 2E) can be deconvoluted into several single peaks corresponding to C-N(P)-C (~286 eV) and C-S-C (283.9 eV),[20,63,64] further confirming that N, S, and P heteroatoms have been doped into the graphene framework. Till now, steroidal alkaloid, nicotine, Ethiopian, tonka bean compounds and so on, which are rich in N, S and other elements, have been isolated from Eclipta prostrata (Scheme 1). Therefore, during the pyrolysis of Eclipta prostrata at high temperature, N-, S-, P-tridoped carbon structures were gradually formed. To the best of our knowledge this is the first report of N-, S-, and P-tridoped carbon nanorings using natural Eclipta prostrata as the single precursor. The surface textural characteristics of the sample were estimated by N_2 adsorption-desorption isotherms. From Fig. 2F, the hysteresis can be seen between adsorption and desorption branches, which shows the emerging mesopores.[65] On the contrary, the corresponding pore-size distribution at high pressure was assessed by the Barret-Joyner-Halenda (BJH) model according to the desorption branch. The detailed data were summarized in Table S1. The mesopore and macropore sizes in the material range from 5 to 30 nm and 100 to 150 nm, respectively (the inset of Fig. 2F). These pores are expected to facilitate the diffusion of reactants in the ORR process.[66,67]

To assess the ORR electrocatalytic properties of these N-, S- and P-tridoped WWCNRs, cyclic voltammograms (CVs) were measured in N_2- or O_2-saturated 0.1 M KOH solution. Comparative studies were performed for bare glassy carbon (GC) and commercial 20 wt% Pt/C (JM). As shown in Fig. 3A, a quasi-rectangular voltammogram without obvious redox peak was observed for the N_2-saturated solution, as a result of the typical supercapacitance effect on porous carbon materials.[30,68] In contrast, a well-defined characteristic ORR peak, centered at −0.078 V with a reaction current of 0.897 mA cm^{-2}, was observed when O_2 was introduced (green curve in Fig. 3A). Notably, the peak potential of the sample catalyst is more positive than that of bare GC (black curve in Fig. 3A) and other recently reported metal-free ORR catalysts such as N-graphene,[69] S-graphene,[21] g-C_3N_4/C,[20] and co-doped graphenes,[59] and is slightly negative compared with the commercial Pt/C catalyst (−0.033 V) (red curve in Fig. 3A), indicating a more facile ORR process with this tridoped sample.

On further study into ORR processes of the sample, linear sweep voltammograms (LSVs) were performed on a rotating-disk electrode (RDE) with different rotating speeds from 400 to 2025 rpm in O_2-saturated 0.1 M KOH solution (Fig. 3B). For the purpose of comparison, analogous LSV curves were obtained for commercial 20 wt % Pt/C (Fig. 3C). As seen from Fig. 3B-C, the current density

Journal Name

ARTICLE

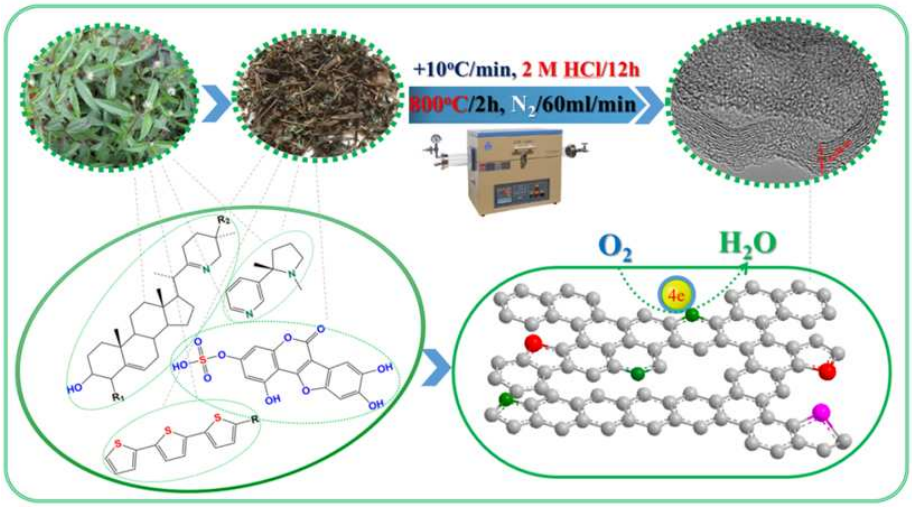

Scheme 1. Illustration of the procedure for the fabrication of N-, S- and P-tridoped WWCNRs from organic-rich worst weed, *Eclipta prostrata*.

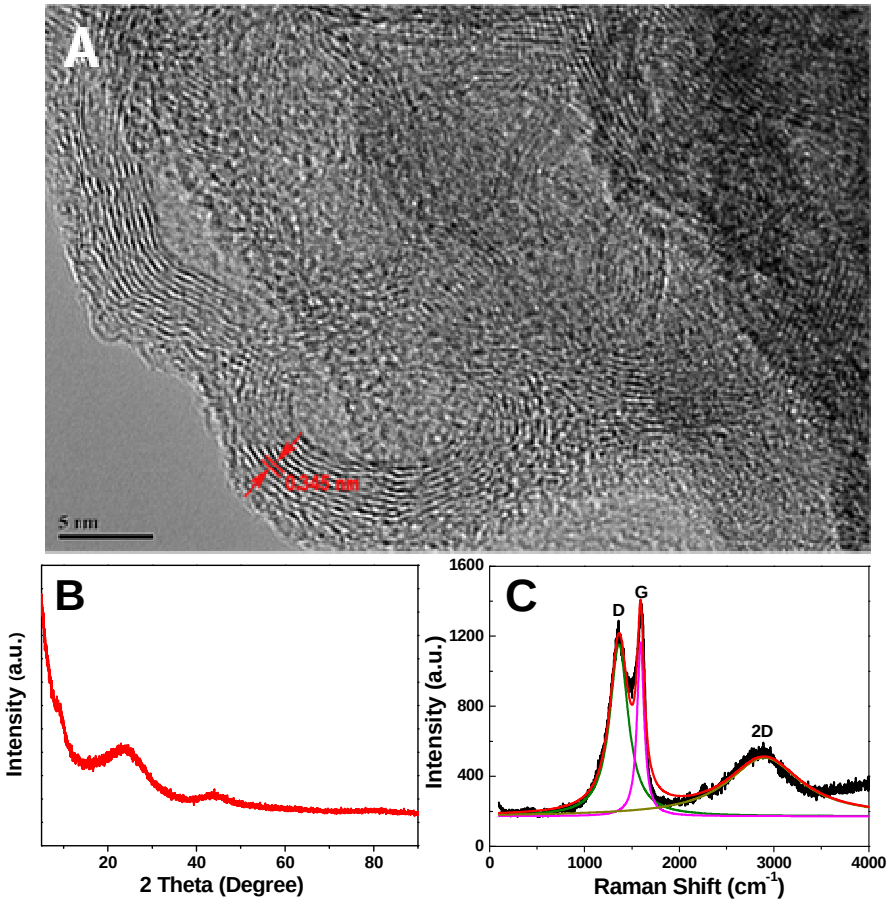

Fig. 1 (A) HRTEM image, (B) XRD pattern over the 2θ range of 5°–90°, and (C) Raman spectrum of WWCNRs with deconvolution into 3 contributions.

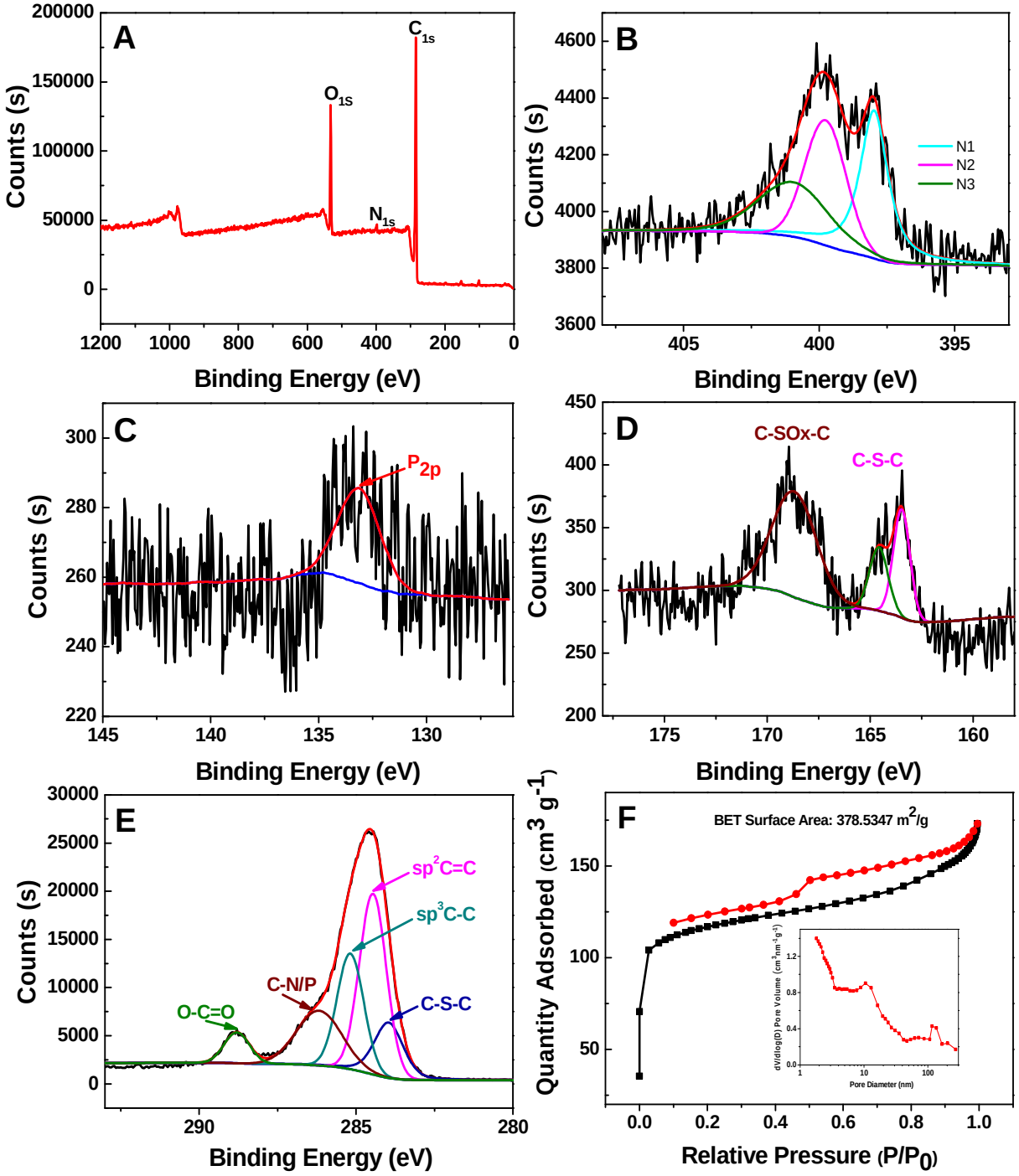

Fig. 2 Full-scan XPS (A), high resolution N1s (B), P2p (C), S2p (D), and C1s (E) XPS scan, and N_2 adsorption-desorption isotherms (F) of WWCNRs. The inset in F is the pore-size distribution of WWCNRs.

Journal Name

ARTICLE

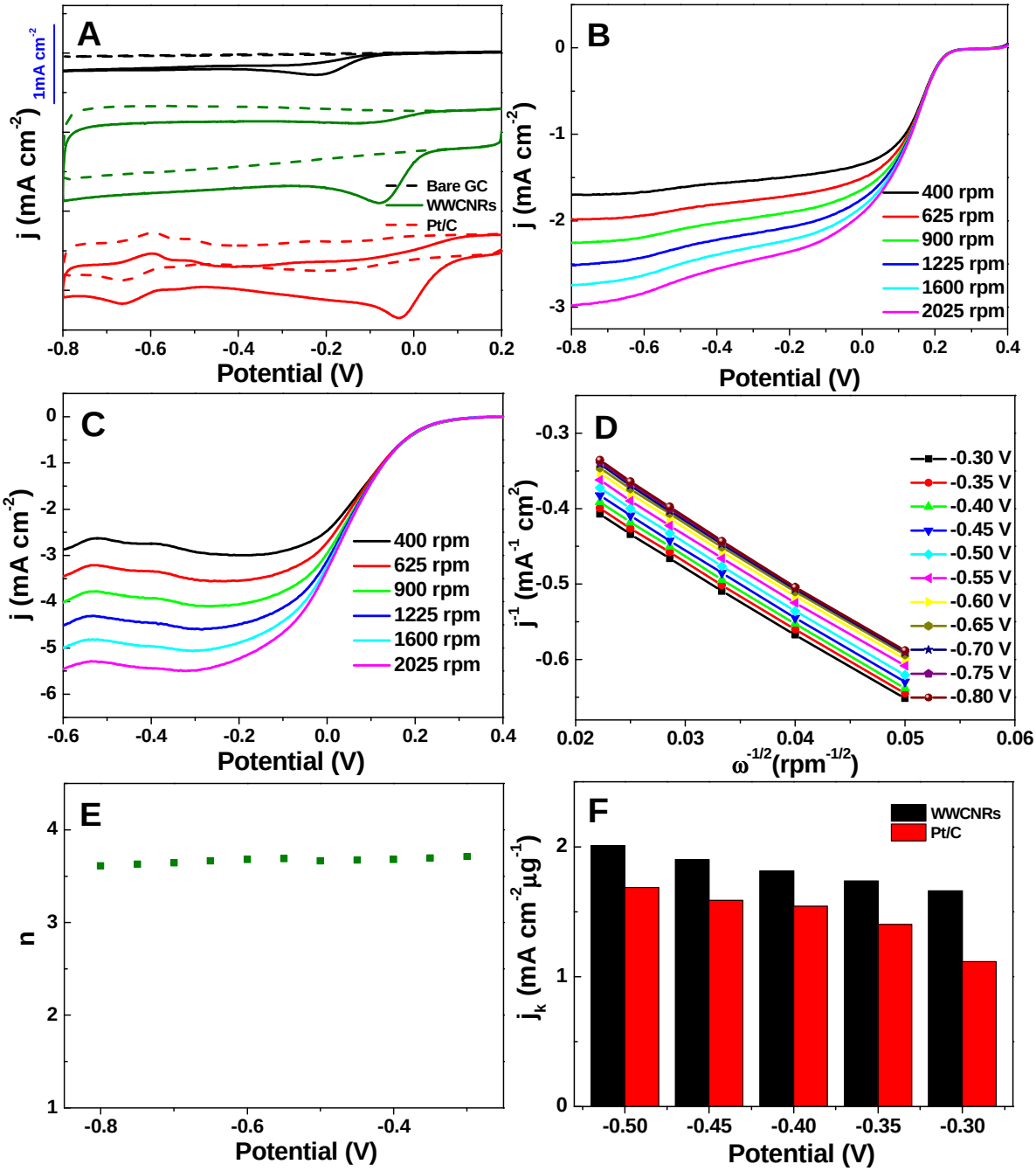

Fig. 3 (A) CV curves of bare GC, WWCNRs, Pt/C in N_2-saturated (dash lines), O_2-saturated (solid lines) 0.1 M KOH solution at a scan rate of 10 mV s^{-1}. (B) RDE curves for WWCNRs and (C) 20 wt% Pt/C in 0.1 M KOH solution at a scanning rate of 10 mV s^{-1} at different rotation speeds. (D) K-L plots for the ORR in O_2-saturated 0.1 M KOH solution for WWCNRs. (E) The electron number calculated from K-L plots. (F) J_k value of WWCNRs and Pt/C calculated from K-L plots (corrected for heteroelement content).

increased with increasing rotation rate from 400 to 2025 rpm resulting from the facilitated transport of electrolytes. Typically, the current simultaneously increased as the potential became more negative, which is commonly observed for metal-free ORR catalysts with mesopores.[20] Remarkably, in terms of onset potential, this is about 0.25 V at 1600 rpm for the sample catalyst, which is more positive than that of most of the currently reported metal-free ORR electrocatalysts (Table S2), very close to the commercial Pt/C catalyst (0.30 V).

To qualify the ORR process on this novel tridoped carbon catalyst, the corresponding Koutecky-Levich (K-L) plots (J^{-1} vs, $\omega^{-1/2}$) were obtained over the electrode potential range from −0.3 to −0.8 V at various rotation speeds. They show good linearity, implying first-order reaction kinetics toward O_2 reduction within the potential range (Fig. 3D). The electron-transfer numbers (n) at different potentials can be calculated according to the slopes of the linear fitted K-L plots on the basis of the K-L equation (Fig. 3E),[21] which is described in the experiment section. The calculated n values of the sample are 3.6-3.8 for potentials between −0.3 and −0.8 V, indicating a favored $4e^-$ pathway of a smooth and electrochemically stable ORR process, with water as the main product. Significantly, the kinetic limiting current density J_k value (corrected for heteroatom content) of WWCNRs exceeded that of commercial Pt/C. E.g., the J_k value of the sample increased from 1.66 mA cm^{-2} g^{-1} to 2.01 mA cm^{-2} g^{-1} as the potential varied from −0.3 V to −0.5 V (Fig. 3F) and its value became nearly 1.5 times as high as that of Pt/C (1.66 mA cm^{-2} g^{-1} vs. 1.11 mA cm^{-2} g^{-1} at −0.3 V), which is a good indication that the current can be improved even further through structural modification.

High selectivity and durability of electrocatalysts for ORR are critical for practical applications. In this study, the tolerance of the sample to methanol crossover was assessed in comparison with that of the commercial Pt/C catalyst. As shown in Fig. 4A, there one new peak characteristic of methanol reduction/oxidation attributed to methanol poisoning of the cathode catalyst (Fig. 4B). This reflects that the sample catalyst has an excellent ability for avoiding methanol crossover, significantly superior to that of the commercial Pt/C catalyst. Fig. 4C was plotted to evaluate the tolerance of the sample toward CO. After introduction of CO, the sample only loses < 7% of its original activity over 4000 s of continuous ORR, while more than 30% of the original activity of 20 wt% Pt/C is lost over 4000 s of continuous ORR, due to the dissociation of the Pt nanoparticles from the carbon substrate or the aggregation of the Pt nanoparticles during the electrochemical processes.[70-75] The durability of the sample and Pt/C was also evaluated. Fig. 4D indicates the resulting current-time (i-t) chronoamperometric response for the sample in 0.1 M KOH with continuous oxygen reduction at −0.3 V (vs. Hg/HgO). Compared with the 87% current retention at the commercial Pt/C electrode after 10,000 s,[76] 94% of the initial current could still persist for our electrode after 18,000 s. The higher stability of the metal-free catalyst can be attributed to the strongly bonded heteroatoms and the improved chemical and mechanical stability of our catalyst relative to that of the carbon-black-based Pt/C, which could effectively prevent the loss of active sites.[40] The remarkably better stability makes our catalyst as a potent candidate for ORR, especially for methanol alkaline fuel cells.

In order to further evaluate the influence of the carbonization temperature on ORR, carbonization procedures of worst weed, Eclipta prostrata, were carried out at 600, 700 and 900 °C (denoted as S-600, S-700 and S-900), respectively. The CVs and LSVs were measured to investigate their ORR activities, respectively. Fig. S2-S11 and Table S1 show the structural and ORR characterizations, demonstrating that WWCNRs produced at 800 °C exhibit the most positive peak potential and onset potential for the ORR among the total four samples, indicating that WWCNRs provide the most excellent electrocatalytic activity. Electrical conductivity and active sites are two main factors affecting the 4-electron reduction of molecular oxygen. Higher pyridine, pyrrole nitrogen contents, and moderate sulfur and phosphorus contents would increase the number of active sites. Higher active site quantity (higher pyridine and pyrrole nitrogen content, Table S1) at 600 and 700 °C carbonization temperature, but poor conductivity (lower graphitization degree); Higher conductivity (higher graphitization degree) at 900 °C, but lower active site quantity (lower pyridine and pyrrole nitrogen content, Table S1). Hence, the optimum temperature appeared to be 800 °C.

Conclusions

In summary, we have described the first design and preparation of N-, S- and P-tridoped WWCNRs as a metal-free ORR catalyst from worst weed, Eclipta prostrata. This novel material shows excellent catalytic activity including a highly positive onset potential and high kinetic limiting current, which makes it closely competitive with the commercial Pt/C catalyst. Our catalyst also shows a high fuel tolerance and much better long-term stability than Pt/C in alkaline environment. This environmentally friendly synthesis of multi-heteroatom-doped carbon materials derived from organic-rich worst weed is simple, low-cost, and easily conducted, which meets the challenge to produce value-added functional carbon with an efficient strategy from cheap and renewable resources. Moreover, the absence of any chemical or physical activation simplifies the procedure and lowers the cost, thus, it is easily adaptable for large-scale synthesis. Because of all these outstanding features, it is expected that the WWCNRs will be a very suitable catalyst for next-generation fuel cells. The work provides a new avenue for the development of multi-heteroatom doped carbon materials using worst weed as the starting materials for fuel cell applications and other areas such as in lithium-air batteries, photocatalysis, oxygen sensors, and water treatment.

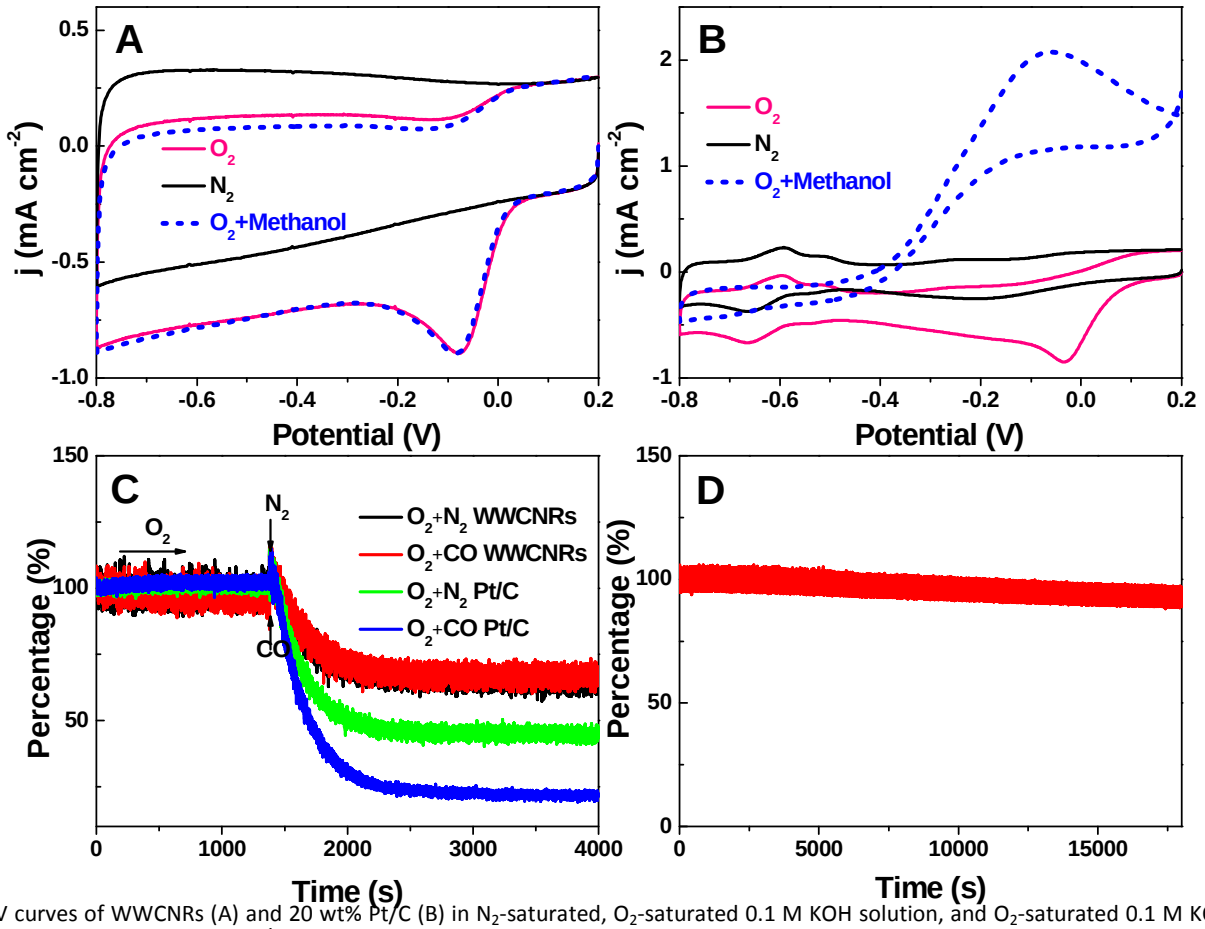

Fig. 4 CV curves of WWCNRs (A) and 20 wt% Pt/C (B) in N_2-saturated, O_2-saturated 0.1 M KOH solution, and O_2-saturated 0.1 M KOH with methanol at a scan rate of 10 mV s^{-1}. (C) The percentage of current density (j) vs. time chronoamperometric responses obtained for 20 wt% Pt/C and WWCNRs electrodes at −0.30 V in O_2-saturated 0.1 M KOH. The arrow indicates the introduction of N_2 or CO into the electrolyte. (D) Stability evaluation of WWCNRs for 18 000 s in an O_2-saturated 0.1 M KOH solution at −0.3 V.

Acknowledgements

Support from the National Science Foundation of China (21471048 and 21071047), the Program for Innovative Research Team in University of Henan Province (No. 14IRTSTHN005), the Program for New Century Excellent Talents in University of Ministry of Education of China (NCET-11-0944), the Excellent Youth Foundation of Henan Scientific Committee (124100510004), the Research Project of Chinese Ministry of Education (No. 213023A), and the Program for Science & Technology Innovation Talents in Universities of Henan Province (2011HASTIT010) is gratefully acknowledged.

Notes and references

1 E. M. Erickson, M. S. Thorum, R. Vasic, N. S. Marinkovic, Frenkel, A. A. Gewirth and R. G. Nuzzo, J. Am. Chem. Soc., 2012, **134**, 197-200.
2 B. C. Steele and H. A. Heinzel, *Nature,* 2001, **414**, 345-352.
3 Y. H. Bing, H. S. Liu, L. Zhang, D. Ghosh and J. J. Zhang, *Chem. Soc. Rev.,*2010, **39**, 2184-2202.
4 M. K. Debe, *Nature,* 2012, **486**, 43-51.
5 M. Nesselberger, M. Roefzaad, R. F. Hamou, P. U. Biedermann,F.F. Schweinberger, S. Kunz, K. Schloegl, G. K. H. Wiberg, S. Ashton, U. Heiz, K. J. J. Mayrhofer and M. Arenz, *Nat. Mater.,* 2013, **12**, 919-924.
6 A. Anastasopoulos, J. C. Davies, L. Hannah, B. E. Hayden, C. E. Lee, C. Milhano, C. Mormiche and L. Offin, *ChemSusChem,* 2013, **6**, 1973-1982.
7 J. Wu, M. Shi, X. Yin and H. Yang, *ChemSusChem,* 2013, **6**, 1888-1892.
8 X. Zhao, M. Yin, L. Ma, L. Liang, C. P. Liu, J. H. Liao, T. H. Lu and W. Xing, *Energy Environ. Sci*., 2011, **4**, 2736-2753.
9 S. I. Choi, S. F. Xie, M. H. Shao, J. H. Odell, N. Lu, H. C. Peng, L. Protsailo, S. Guerrero, J. Park, X. H. Xia, J. G. Wang, M. J. Kim and Y. N. Xia, *Nano Lett.,* 2013, **13**, 3420-3425.
10 K. Cai, J. W. Liu, H. Zhang, Z. Huang, Z. C. Lu, M. F. Foda, T. T. Li and H. Y. Han, *Chem. Eur. J.,* 2015, **21**, 7556-7561.
11 D. L. Wang, H. L. Xin, R. Hovden, H. S. Wang, Y. C. Yu, D. A. Muller, F. J. DiSalvo and H. D. Abruña, *Nat. Mater.,* 2013, **12**, 81-87.
12 J. H. Jang, E. Lee, J. Park, G. Kim, S. Hong and Y. U. Kwon, *Sci. Rep*., 2013, **3**, 28721-28728.
13 R. Silva, D. Voiry, M. Chhowalla and T. Asefa, *J. Am. Chem. Soc.,* 2013, **135**, 7823-7826.
14 M. Lefevre, E. Proietti, F. Jaouen and J. P. Dodelet, *Science,* 2009, **324**, 71-74.
15 J. B. Xu, P. Gao and T. S. Zhao, *Energy Environ. Sci.,* 2012, **5**, 5333-5339.
16 I. Roche, E. Chainet, M. Chatenet and J. Vondrak, *J. Phys. Chem., C* 2007, **111**, 1434-1443.
17 W. Zhang, Z. Y. Wu, H. L. Jiang and S. H. Yu, *J. Am. Chem. Soc.,* 2014, DOI: 10.1021/ja5084128.
18 Y. Liang, Y. Li, H. Wang, J. Zhou, J. Wang, T. Regier and H. Dai, *Nat. Mater.,* 2011, **10**, 780-786.

19 K. Gong, F. Du, Z. Xia, M. Durstock and L. Dai, *Science,* 2009, **323**, 760-764.
20 Y. Zheng, Y. Jiao, J. Chen, J. Liu, J. Liang, A. Du, W. Zhang, Z. Zhu, S. C. Smith, M. Jaroniec, G. Q. Lu and S. Z. Qiao, *J. Am. Chem. Soc.,* 2011, **133**, 20116-20119.
21 M. R. Gao, Z. Y. Lin, J. Jiang, C. H. Cui, Y. R. Zheng and S. H. Yu, *Chem. Eur. J.,* 2012, **18**, 8423-8429.
22 L. Qu, Y. Liu, J. B. Baek and L. Dai, *ACS Nano,* 2010, **4**, 1321-1326.
23 L. Yang, S. Jiang, Y. Zhao, L. Zhu, S. Chen, X. Wang, Q. Wu, J. Ma, Y. Ma and Z. Hu, *Angew. Chem.* 2011*,* **123***,* 7270-7273; *Angew. Chem. Int. Ed.,* 2011, **50**, 7132-7135.
24 L. Lai, J. R. Potts, D. Zhan, L. Wang, C. K. Poh, C. Tang, H. Gong, Z. Shen, J. Lin and R. S. Ruoff, *Energy Environ. Sci.,* 2012, **5**, 7936-7942.
25 J. Zhang, Y. Chen and X. Wang, *Energy Environ. Sci.*, 2015, DOI: 10.1039/C5EE01895A.
26 T. Y. Wang, D. L. Gao, J. Q. Zhuo, Z. W. Zhu, P. Papakonstantinou, Y. Li and M. X. Li, *Chem. Eur. J.,* 2013, **19**, 11939-11948.
27 Y. Zhao, L. J. Yang, S. Chen, X. Z. Wang, Y. W. Ma, Q. Wu, Y. F. Jiang, W. J. Qian and Z. Hu, *J. Am. Chem. Soc.,* 2013, **135**, 1201-1204.
28 Y. Zheng, J. Liu, J. Liang, M. Jaroniec and S. Z. Qiao, *Energy Environ. Sci.,* 2012, **5**, 6717-6731.
29 W. Xiong, F. Du, Y. Liu, A. Perez, Jr. M. Supp, T. S. Ramakrishnan, L. M. Dai and L. Jiang, *J. Am. Chem. Soc.,* 2010, **132**, 15839-15841.
30 Y. L. Zhu, C. Su, X. M. Xu, W. Zhou, R. Ran and Z. P. Shao, *Chem. Eur. J.,* 2014, **20**, 15533-15542.
31 Y. Zheng, Y. Jiao, M. Jaroniec, Y. Jin and S. Z. Qiao, *Small,* 2012, **8**, 3550-3566.
32 L. Y. Feng, L. Q. Yang, Z. J. Luo, M. Li, D. B. Wang and Y. G. Chen, *Sci. Rep.,* 2013, **3**, 33061-33068.
33 P. Pachfule, V. M. Dhavale, S. Kandambeth, S. Kurungot and R. Banerjee, *Chem. Eur. J.,* 2013, **19**, 974-980.
34 Z. W. Liu, F. Peng, H. J. Wang, H. Yu, W. X. Zheng and J. Yang, *Angew. Chem. Int. Ed.,* 2011, **50**, 3257-3261.
35 D. S. Yang, D. Bhattacharjya, S. Inamdar, J. Park and J. S. Yu, *J. Am. Chem. Soc.,* 2012, **134**, 16127-16130.
36 C. Zhang, N. Mahmood, H. Yin, F. Liu and Y. Hou, *Adv. Mater.,* 2013, **25**, 4932- 4937.
37 J. P. Paraknowitsch and A. Thomas, *Science,* 2013, **6**, 2839-2855.
38 Y. Z. Su, Y. Zang, X. D. Zhuang, S. Li, D. Q. Wu, F. Zhang and X. L. Feng, *Carbon,* 2013, **62**, 296-301.
39 J. Liang, Y. Jiao, M. Jaroniec and S. Z. Qiao, *Angew. Chem. Int. Ed.,* 2012, **51**, 11496-11500.
40 X. X. Yang, H. J. Wang, J. Li, W. X. Zheng, R. Xiang, Z. K. Tang, H. Yu and F. Peng, *Chem. Eur. J.,* 2013, **19**, 9818-9824.
41 S. B. Yang, L. J. Zhi, K. Tang, X. L. Feng, J. Maier and K. Müllen, *Adv. Funct. Mater.,* 2012, **22**, 3634-3640.
42 N. R. Sahraie, J. P. Paraknowitsch, C. Göbel, A. Thomas and P. Strasser, *J. Am. Chem. Soc.,* 2014, **136**, 14486–14497.
43 X. Wang, J. Wang, D. Wang, S. Dou, Z. Ma, J. Wu, L. Tao, A. Shen, C. Ouyang, Q. Liu and S. Wang, *Chem. Commun.,* 2014, **50**, 4839-4842.
44 D. C. Higgins, M. A. Hoque, F. Hassan, J.-Y. Choi, B. Kim and Z. Chen, *ACS Catal.,* 2014, **4**, 2734-2740.
45 W. Ai, Z. M. Luo, J. Jiang, J. H. Zhu, Z. Z. Du , Z. X. Fan , L.H. Xie, H. Zhang, W. Huang and T. Yu, *Adv. Mater.*, 2014, **26**, 6186-6192.
46 J. Wu, Z. R. Yang, X. W. Li, Q. J. Sun, C. Jin, P. Strasserd and R. Z. Yang, *J. Mater. Chem. A*, 2013, **1**, 9889-9896.
47 C. H. Choi, S. H.Park and S. I. Woo, *ACS Nano,* 2012, **6**, 7084-7091.
48 C. H. Choi, S. H. Park and S. I. Woo, *J. Mater. Chem.*, 2012, **22**, 12107-12115.
49 J. Liu, P. Song, Z. G. Ning and W. L. Xu, *Electrocatalysis*, 2015, **6**,132-147.
50 Z. L. Ma, S. Dou, A. L. Shen, L. Tao, L. L. Dai and S. Y. Wang, *Angew. Chem. Int. Ed.*, 2014, **53**, 1- 6.
51 P. Song, X. J. Bo, A. Nsabimana and L. L. Guo, *Int. J. Hydrogen Energy*, 2014, **39**, 15464-15 473.
52 C. H. Choi, M. W. Chung, S. H. Park and S. I. Woo, *Phys. Chem. Chem. Phys*., 2013, **15**, 1802-1805.
53 X. H. Lin, Y. B. Wu, S. Lin, J. W. Zeng, P. Y. Zeng and J. Z. Wu, *Molecules,* 2010, **15**, 241-250.
54 G. Rajakumar and A. A. Rahuman, *Acta Tropica,* 2011, **118**, 196-203.
55 H. T. Yu, Y. C. Li, X. H. Li, L. Z. Fan and S. H. Yang, *Chem. Eur. J.,* 2014, **20**, 3457-3462.
56 C. Hu, Y. Xiao, Y. Zhao, N. Chen, Z. Zhang, M. Cao and L. Qu, *Nanoscale,* 2013, **5**, 2726-2733.
57 S. Lim, S. H. Yoon, I. Mochida and D. H. Jung, *Langmuir,* 2009, **25**, 8268-8273.
58 Y. Li, J. Wang, X. Li, J. Liu, D. Geng, J. Yang, R. Li and X. Sun, *Electrochem. Commun.,* 2011, **13**, 668-672.
59 X. Y. Liu, G. T. Fu, Y. Chen, Y. W. Tang, P. L. She and T. H. Lu, *Chem. Eur. J.,* 2014, **20**, 585-590.
60 P. P. Su, H. Xiao, J. Zhao, Y. Yao, Z. G. Shao, C. Li and Q. H. Yang, *Chem. Sci.,* 2013, **4**, 2941-2946.
61 Z. K. Zhao, Y. T. Dai, G. F. Ge and G. R. Wang, *Chem. Eur. J.,* 2015, **21**, 8004-8009.
62 J. Xu, G. Dong, C. Jin, M. Huang and L. Guan, *ChemSusChem,* 2013, **6**, 493-499.
63 S. Wan, L. Wang and Q. Xue, *Electrochem. Commun.,* 2010, **12**, 61-65.
64 J. Liang, Y. Zheng, J. Chen, J. Liu, D. Hulicova-Jurcakova, M. Jaroniec and S. Z. Qiao, *Angew. Chem. Int. Ed.,* 2012, **51**, 3892-3896.
65 S. Wang, D. Yu, L. Dai, D. W. Chang and J.-B. Baek, *ACS Nano,* 2011, **5**, 6202-6209.
66 S. Yang, X. L. Feng, X. C. Wang and K. Müllen, *Angew. Chem. Int. Ed.,* 2011, **50**, 5339-5343.
67 H. L. Jiang, Y. H. Zhu, Q. Feng, Y. H. Su, X. L. Yang and C. Z. Li, *Chem. Eur. J.,* 2014, **2**, 3106-3112.
68 Y. Xiao, C. G. Hu, L. T. Qu, C. W. Hu and M. H. Cao, *Chem. Eur. J.,* 2013, **19**,14271-14278.
69 S. Yang, L. Zhi, K. Tang, X. Feng, J. Maier and K. Müllen, *Adv. Funct. Mater.,* 2012, **22**, 3634-3640.
70 H. Uchida, K. Izumi and M. Watanabe, *J. Phys. Chem. B,* 2006, **110**, 21924-21930.
71 H. J. Lee, M. K. Cho, Y. Y. Jo, K. S. Lee, H. J. Kim, E. Cho, S. K. Kim, D. Henkensmeier, T. H. Lim and J. H. Jang, *Polym. Degrad. Stab.,* 2012, **97**, 1010-1016.
72 Y. Yu, H. L. Xin, R. Hovden, D. Wang, E. D. Rus, J. A. Mundy, D. A. Muller and H. D. Abruña, *Nano Lett.,* 2012, **12**, 4417-4423.
73 Y. Zhang, Q. Huang, Z. Zou, J. Yang, W. Vogel and H. Yang, *J. Phys. Chem. C,* 2010, **114**, 6860-6868.
74 Q. Ge, S. Desai, M. Neurock and K. Kourtakis, *J. Phys. Chem. B,* 2001, **105**, 9533-9536.
75 A. G. Kong, B. Dong, X. F. Zhu, Y. Y. Kong, J. L. Zhang and Y. K. Shan, *Chem. Eur. J.,* 2013, **19**, 16170-16175.
76 S. Gao and K. Geng, *Nano Energy,* 2014, **3**, 44-50.

A table of contents entry

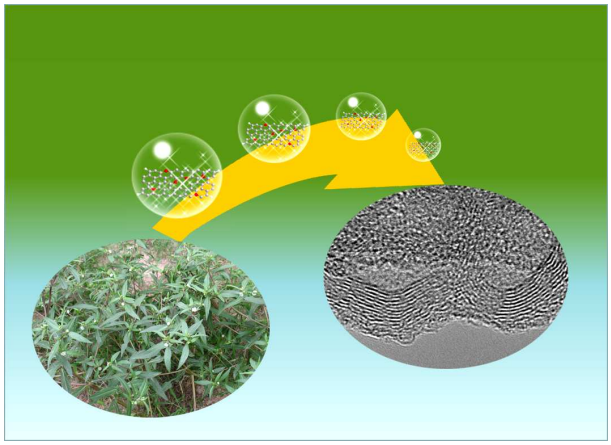

N-, S-, and P-tridoped carbon nanorings are sustainably derived from worst-weed that can serve as metal-free and selective ORR electrocatalyst.